

DOI: 10.1007/s11430-006-0242-7

Origin of natural sulphur-bearing immiscible inclusions and H₂S in oolite gas reservoir, Eastern Sichuan

LIU Dehan, XIAO Xianming, XIONG Yongqiang, GENG Ansong, TIAN Hui, PENG Ping'an, SHEN Jiagui & WANG Yunpeng

State Key Laboratory of Organic Geochemistry, Guangzhou Institute of Geochemistry, Chinese Academy of Sciences, Guangzhou 510640, China

Correspondence should be addressed to Liu Dehan (email: liudh@gig.ac.cn)

Received June 3, 2005; accepted August 11, 2005

Abstract Based on results of microscopic observation and laser Raman analysis about fluid inclusions, multiple special forms of immiscible inclusions that contain sulphur, liquid hydrocarbon, bitumen, *etc.* were discovered in samples collected from the H₂S gas reservoir-containing carbonates in the Lower Triassic Feixianguan Formation in the Jinzhu-Luojia area, Kai County, Sichuan Province. Based on the lithology and burial history of the strata involved as well as measurement results of homogenization temperature of fluid inclusions, bitumen reflectivity, *etc.*, it is concluded that the H₂S in the gas reservoir resulted from the thermal reaction between hydrocarbons in reservoir and CaSO₄ in the gypsum-bearing dolostone section at the high temperature (140°C—170°C) oil-cracked gas formation stage in Late Cretaceous. Thereafter, research on a great number of immiscible inclusions in the reservoir reveals that elemental sulphur resulted from oxidation of part of the earlier-formed H₂S and further reaction between sulphates, hydrocarbons and H₂S in geological fluids in H₂S-bearing gas reservoir at a temperature of 86°C—89°C and a pressure of 340×10⁵Pa and during the regional uplift stage as characterized by temperature decrease and pressure decrease in Tertiary. Meanwhile, gypsum, anhydrite and calcite formed at this stage would trap particles like elemental sulphur and result in a variety of special forms of immiscible inclusions, and these inclusions would contain information concerning the complexity of the fluids in the reservoir and the origin of H₂S and natural sulphur in the gas reservoir.

Keywords: Sichuan Basin, immiscible inclusion, origin of hydrosulfide, natural sulphur, oil-cracking gas, microscopic laser Raman analysis.

Fluid inclusions as captured in homogeneous fluids in rocks and minerals have been extensively studied and successfully applied to exploring the metallogenic temperature and pressure of metallic ore deposits and in investigating hydrocarbon generation, migration, *etc.*^[1–6]. In regard to multiple forms of immiscible inclusions in rocks and minerals, a significant

amount of research has already been conducted toward the immiscible inclusions and “boiling” inclusions in CO₂-H₂O system, only study on immiscible inclusions of other formation mechanisms is obviously lacking. At present, fluid inclusion study in the field of hydrocarbon geological research is mainly focused on homogenization temperature, freezing point temperature,

etc. of fluid inclusions as trapped in homogenized system, while few research on immiscible inclusions has been published so far. As a matter of fact, multiple forms of immiscible inclusions might occur in some hydrocarbon reservoirs and pervious layers, only not much focus was put on their research. Recently the authors discovered the occurrence of polyphase immiscible inclusions that contain natural sulphur and H₂S in the Ertan gas reservoir of the Triassic Feixianguan Formation in Sichuan Basin, which can undoubtedly yield key information concerning the origin of hydrogen sulfide and natural sulphur. Gas from the Ertan reservoir is highly enriched in H₂S, and on December 23, 2003 a blowout accident occurred in the LuoJia Village 16 gas mine in Kai County, Sichuan, which resulted in large area H₂S-related poisoning. Therefore, study on the origin of hydrogen sulfides and natural sulphur in gas reservoirs has become a key issue that has attracted extensive attention in gas exploration and development.

1 Samples and petroleum geologic setting

1.1 Petroleum geologic setting

The oolite gas reservoir in the Feixianguan Formation is located in Kaijiang, Liangping, Kaixian and Wanyuan in northeast Sichuan, and geotectonically belongs to the northwestern margin of the Yangtze Plate. Its basement is composed of Proterozoic low metamorphic rocks and small amount of acidic eruptive rocks, and on this basement, Sinian to Tertiary strata ca. 12,000 m thick were deposited, among which the Sinian system to Middle Triassic Leikoupo Formation mainly consist of carbonates of shallow sea facies and small a amount of deposits of oceanic-continental transitional facies and have a thickness of ca. 4,000—7,000 m, while the Middle Triassic Xujiahe Formation and its overlying strata mainly consist of clastic rocks of terrestrial facies^[7].

Petrographical and paleogeographical study and palaeotectonic stress field analysis indicate that multiple syncline, depression and antecline structures were developed due to the pullapart extension of Sichuan Basin ever since Paleozoic. In the study area, the NE-trending Kaijiang-Liangping trough formed in Late Permian to early Triassic controlled the deposi-

tion of sapropel-type pelitic carbonate source rocks of trough facies in Permian and Triassic, and the layout of the Ertan gas reservoir in the Feixianguan Formation in the two sides of the trough. Here in Eastern Sichuan, the marine facies strata were mainly developed from Upper Permian to Lower Triassic, and the Lower Triassic Feixianguan Formation mainly consists of pelitic carbonates of marine facies-tidal-flat facies and saltish lagoon facies and deposits of gypsum-salt facies. The pelitic carbonates of trough facies in the Upper Permian Changxing Formation has a relic organic carbon concentration being as high as 0.4%—1.1%, while the pelitic carbonates of trough facies in Feixianguan Formation has a relic organic carbon concentration of 0.4%—0.5%, hence becoming major hydrocarbon source rocks in the study area. On the two sides of the NE-trending Kaijiang-Liangping trough, carbonate rocks of oolitic beach facies characterized by abundant porosity were developed, and became important hydrocarbon reservoirs. The multiple layers of gypsum-salt and pelitic rocks in the Triassic Jialingjiang Formation and Feixianguan Formation served as the direct covers for the Ertan gas reservoir in the Feixianguan Formation and the Cretaceous red beds as the regional cover for the gas reservoir.

An analysis about the burial history and thermal evolution history of the hydrocarbon source rocks in the Permian System and the Triassic System in the study area was carried out, and the results indicate that at the end of Triassic, the vitrinite reflectivity R_0 is as high as 0.5%—0.7%, signaling the beginning of oil generation stage, while at the sedimentation stage of the Lower Shaximiao Formation in the Early Jurassic-Mid-Jurassic system, the vitrinite reflectivity R_0 can be as high as 0.7%—1.0%. Thereafter, sedimentation and settlement were speeded up, and at the sedimentation stage of Late Jurassic Suining Formation, the vitrinite reflectivity R_0 of hydrocarbon source rocks became 1.0%—1.3%, signaling the peak period for oil generation. At the sedimentation stage of Late Jurassic Penglai Formation, the maturity R_0 for hydrocarbon source rocks was 1.3%—2.0%, signaling the stage for condensate oil and wet gas formation; Cretaceous to Early Miocene is the stage for maximum settlement, at this stage the thermal evolution degree for source rocks and reservoirs R_0 was as high

as 2.5%—3%, signaling the beginning of the stage for the formation of oil-cracked gas and dry gas. At this stage the study area shows an average geothermal gradient of 3.01°C/100 m, the maximum Tertiary burial depth of ca. 6,400 m and the highest geothermal temperature of ca. 220°C. After this stage, the hydrocarbon reservoir in the study area was at the process of pressure decrease and temperature decrease due to the extensive uplift of Sichuan Basin in Pliocene^[7,8].

The oolite limestone gas reservoir in Lower Triassic Feixianguan Formation is mainly of the structural-lithological trap type and consists of oolitic dolostones. The reservoir is characterized by development of pores and fissures, and shows high gas maturity, CH₄ content of 73.7%—84.9%, CH₂ content of 0.03%—0.11%, CH₃ content of 0.0%—0.05%, H₂S content of 8.28%—17.06%, CO₂ content of 0.46%—10.41%, N₂ content of 0.42%—1.11%, H₂ content of 0.002%—3.45%, He content of 0.013%—0.03%, and $\delta^{13}\text{C}_1 = -32.35\text{‰}$ — -29.52‰ , $\delta^{13}\text{C}_2 = -33.8\text{‰}$ — -32.39‰ ^[8]. Gas compositions and carbon isotope results for methane and ethane reveal that the gas is of the crude-cracked type. Presently the pressure coefficient for the gas reservoir is 1.03—1.37.

2 Samples and experimental conditions

2.1 Samples

Research was carried out toward nine boreholes located at Luojiashai-Jinzhu, Dukouhe and Tieshan areas on the two sides of Kaijiang-Liangping trough, and dozens of samples were collected from the carbonate reservoirs and source rocks in the Triassic and Permian strata, while our focus was placed on the carbonate reservoir samples showing development of pores and fissures in Lower Triassic (T₁^f³⁻¹) and Upper Permian (P₂²). Distribution of the samples and descriptions of the optical properties of the reservoir bitumen are shown in Fig. 1 and Table 1.

2.2 Experimental conditions

For microscopic observation about inclusions and solid bitumen in reservoir samples, polarizing, reflection and fluorescence systems of LEITZ LABORLUX

12 POL S and LEICA DMR XP, were used respectively. Here the conditions for fluorescence observation are: 100W Hg lamp, excitation wavelength: H3-420—490 nm, dichromatic reflection mirror: RKB-510 nm, protection filter wavelength: 515 nm.

As to the shapes, dimensions and gas/liquid ratios of fluid inclusions, LEICA DC350 digital camera system and QWIN STANDRD image analysis software were used together with LEICA DMR XP-NIKON DXM 1200F digital imaging system.

In regard to measurement of homogenization temperatures and freezing temperatures of fluid inclusions, USGS FLUID INI gas flow stage and LINKAM THMS-G600 stage were respectively used for both heating and freezing, together with objectives L32/0.49 P and H50/0.50 of long focal lengths, and at a heating rate of 1—5°C/m.

In regard to measurement of reflectivity of bitumen in samples, LEITZ MPV 3 microphotometer was used and the operating conditions involve a wavelength of 514nm, objective of 50X/0.85 OIL P, immersion oil with $N=1.515$, and reflectivity calibration standard of NR1149 optical glass with $R_0=1.24\%$.

In regard to microscopic laser Raman analysis about inclusions, RENISHAN (R) RM-2000 model Raman spectrophotometer was used, and the operating conditions are Ar⁺ laser generator with laser wavelength of 514 nm, power of 25.2 mw, grating slit of 20 μm , objective N PLAN 50X/0.75 P, measurement diameter of 5 μm , and scanning time of 10 s.

3 Types and characteristics of occurrence of fluid inclusions

Fluid inclusions are primary samples of geological fluids sealed in authigenic minerals, enlargement edges of minerals or healing surfaces of secondary fissures in minerals during the petrogenetic evolution of rocks and migration-charge processes of hydrocarbons. However, the formation and distribution of various types of fluid inclusions in the reservoir were constrained by multiple geological and geochemical conditions, as the reservoir is characterized by strong petrogenesis, remarkable recrystallization. Hence fluid inclusions were well developed along interfaces among oil, gas and water, while in pure gas reservoir

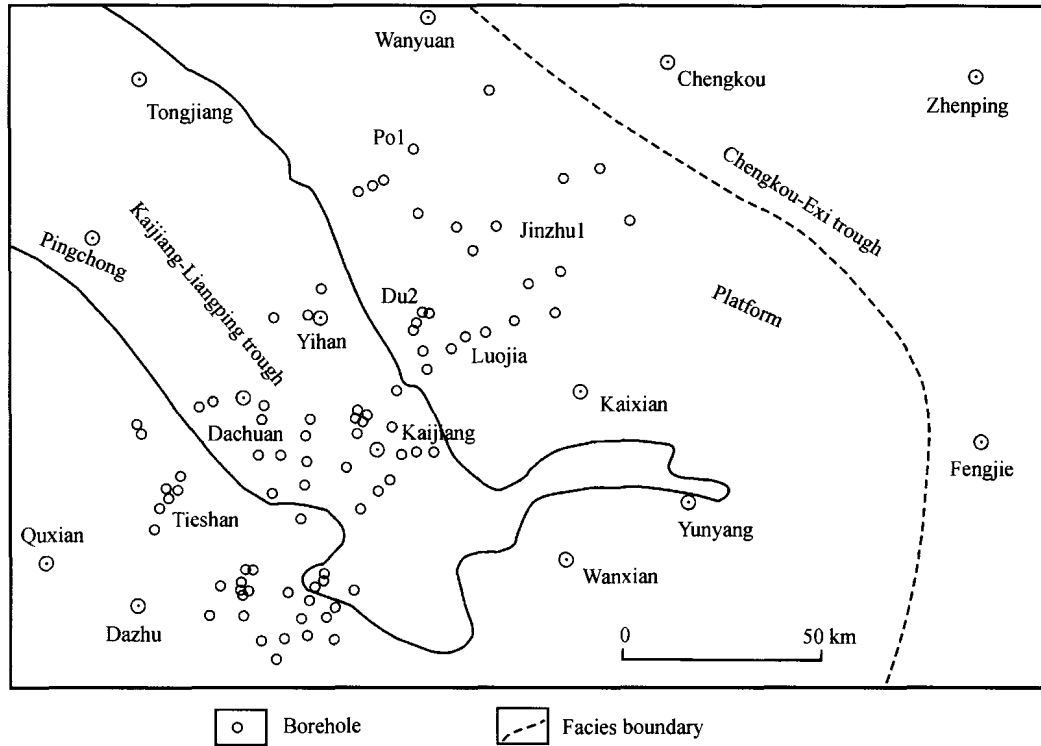


Fig. 1. Plane map about Jinzhu-Luojia region in the Kaijiang-Liangping trough in Sichuan Basin.

Table 1 Descriptions about fluid inclusions in minerals and measurement of reflectivity of reservoir bitumen in samples

Sample	Bore No.	Bore depth (m)	Age	Bitumen type	Bitumen reflectivity (BR ₀ %)	Observation of fluid inclusions
Cd85	Jinzhu 1	2969	T _v ³⁻¹	Carbonate reservoir		Containing immiscible inclusions
Cd86	Jinzhu 1	2977	T _v ³⁻¹	Carbonate reservoir		Containing immiscible inclusions
Cd5	Po 1	3953.56	T _v ³⁻¹	Pyrobitumen in inhomogenized structural reservoir	2.40(2.4—3.10)	
Cd9	Po 2	4034.9	T _v ³⁻¹	Pyrobitumen in inhomogenized structural reservoir	2.42(2.4—2.45)	
Cd20	Po 3	3617.5	T _v ³⁻¹	Pyrobitumen in inhomogenized structural reservoir	4.15(5.87—4.26)	
Cd24	LuoJia 1	3477.7	T _v ³⁻¹	Carbonate reservoir	2.72(2.67—2.76)	Containing fluid inclusions
Cd24	LuoJia 1	3477.7	T _v ³⁻¹	pyrobitumen in inhomogenized structural reservoir	2.72(2.67—2.76)	
Cd27	LuoJia 1	3494	T _v ³⁻¹	pyrobitumen in inhomogenized structural reservoir	3.55(2.95—4.5)	
Cd42	Du 2	4374	T _v ³⁻¹	Carbonate reservoir and carbonates		Containing fluid inclusions
Cd-60	Tieshan5	2874	T _v ³⁻¹	pyrobitumen in inhomogenized structural reservoir	2.52(2.33—2.76)	
Cd-61	Tieshan5	2876	T _v ³⁻¹	pyrobitumen in inhomogenized structural reservoir	2.45(2.19—2.88)	
Cd-58	Tieshan5	3111	P ₂ ²	bitumen in inhomogenized structural reservoir	2.63(2.55—2.83)	
Cd-74	Huanglong 1	4019	P ₂ ²	bitumen in inhomogenized structural reservoir	2.25(2.05—2.45)	
Cd-76	Huanglong 4	3620	P ₂ ²	bitumen in inhomogenized structural reservoir	2.14(1.78—2.32)	

and oil reservoir the development of fluid inclusions was constrained to a great extent.

Due to the complexity of petrogenesis undergone by the reservoirs and formation and evolution of hydrocarbon reservoirs in the study area, fluid inclusions show great inhomogeneity in both type and extent of development. Fluid inclusions were well developed in sparite and dolomite that show apparent recrystallization, in oolitic carbonate cement, in authigenic calcite, dolomite, quartz in carbonate solution holes, and in secondary gypsum-anhydrite in pores of rocks, while fluid inclusions that can be used for temperature measurement were hard to find in finely crystallized carbonate rocks, or in coarse-grained milk-white calcite and dolomite veins. The inclusions distributed in the reservoirs show a variety of types, which include single phase pure liquid inclusions, pure gas inclusions, solid bitumen inclusions, and two-phase gas-liquid inclusions as well as three-phase CO₂-bearing inclusions, *etc.* However, it should be noted that inclusions formed in the early stage were seldom preserved in perfect conditions due to dissolution and deutero-genesis in reservoirs. The inclusions that currently occur in the reservoirs are mainly comprised of early stage inclusions resulted from formation of oil-cracked gas in Yanshannian and late stage inclusions formed during the uplift in Himalayan. In order to investigate the origins of both gas and H₂S, this paper will be focused on inclusions that can reflect the temperature required for formation and evolution of gas and H₂S and immiscible inclusions that contain elemental sulphur and H₂S, *etc.* In regard to the former type of inclusions, they are mainly hosted in minerals like recrystallized calcite and dolomite, and it was found that bitumen inclusions and gas inclusions were generally paragenetic with high temperature fluid inclusions. In regard to the latter type of inclusions, they are mainly hosted in minerals like gypsum-anhydrite and calcite that were formed at later stage, and it was found that gas inclusions, low temperature salt water inclusions and a small quantity of oil inclusions were generally paragenetic with immiscible inclusions.

In regard to two-phase salt water inclusions that were well preserved and show big sizes among fluid inclusions in reservoirs, measurement of their homogenization temperature, initial melting temperature, eutectic temperature and freezing point was performed,

and the results are shown in Table 2 and Fig. 2. Meanwhile, measurement of homogenization temperature and PVTX simulation and calculation were conducted toward oil inclusions that were rarely seen and show yellow fluorescence. As shown in Fig. 2, the homogenization temperature for fluid inclusions in minerals can be approximately classed into three groups: 80°C–120°C, 130°C–160°C, and 170°C–200°C. Here the homogenization temperature for elemental sulphur-bearing immiscible inclusions in gypsum-anhydrite and calcite that were formed at later stage, and for small quantity of oil inclusions mainly varies in the range of 89°C–105°C.

The bitumen reflectivity of Triassic and Permian carbonates is shown in Fig. 3.

4 Types and characteristics of immiscible inclusions

Immiscible inclusions in minerals and rocks can be directly trapped from inhomogenized systems during either petrogenic or metallogenic process, and can also be captured from the originally homogenized system, only in the latter case the inclusions thus captured would be transformed into secondary immiscible inclusions due to a variety of later stage geological processes. An extensive investigation about hydrocarbon reservoir samples collected from the study area indicates that fluid inclusions occur in multiple forms, and our research was focused on immiscible fluid inclusions, which contain hydrocarbon, natural sulphur, H₂S, HS⁻¹ and the results are listed in the following sections (Fig. 4-1–10).

4.1 Liquid hydrocarbon-bearing protogenic immiscible fluid inclusions

Since oil and natural gas both show rather low solubility in water and petroleum hydrocarbons are strongly hydrophobic, systems characterized by the immiscible coexistence of oil, gas and water would generally occur in hydrocarbon reservoir traps and persist during the oil generation and migration processes. Multiple forms of immiscible fluid inclusions would be easily formed in transition zones between oil and water and between gas and water, in milky-cloudy systems and in decompressed “boiling” state.

Table 2 Measurement results of homogenization temperature, initial melting temperature, eutectic temperature and freezing point of fluid inclusions

Sample No.	Drill No.	Drill depth(m)	Age	Host mineral	Th(°C)	Gas/liquid (%)	Freezing point	Initial melting temp.(°C)	Eutectic temp. (°C)
Cd-5	Po 1	3459.9	T _f ³⁻¹		89 95 171 175 176 182 184		-5 -6.5 +3.2	-20	-10 -61
Cd-42	Du 2	4374	T _f ³⁻¹	Dolomite	158 176 161 164 179	11-15			
Cd-426	Du 2	4374	T _f ³⁻¹	Dolomite	151 127 140 162	12-16			
Cd-85	Jinzhū 1	2969	T _f ³⁻¹		102 105 154	6-9 11-16			
Cd-24	Luojia 1	3473.3	T _f ³⁻¹	Calcite	118 120 116	6-8 15-20	-5.5 -10	-20 -23	-90 -85
Cd-86	Jinzhū 1	3012	T _f ³⁻¹	Calcite Anhydrite	94 97 102 105 84.5 89 90 95 94 97 101 105 109 112 115 105 102 114 138 140 148 148 150 157 158 155 156	7.5 8.6 13 16	-5.5 -6	-24.5	-82
Cd-66	Tieshan 5	3094	P ₂ ²	Calcite	108 110 120 180182	9.3 18			
Cd-59	Tieshan 4	3114	P ₂	Calcite	126 194	13			

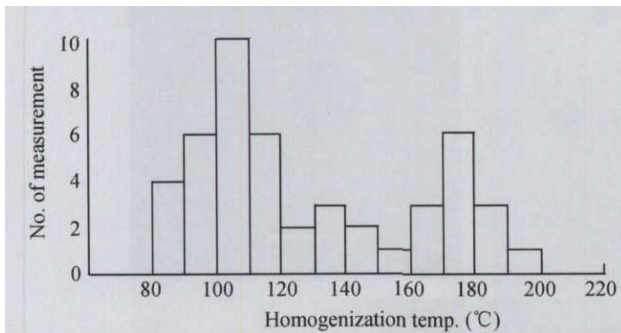
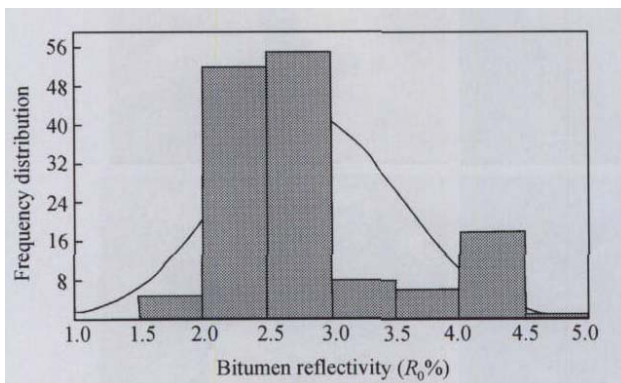
Fig. 2. Histogram showing frequency distribution of homogenization temperature of fluid inclusions in Triassic System (T_f).

Fig. 3. Histogram showing frequency distribution of reflectivity of Triassic and Permian solid bitumen.

In the study area primary immiscible fluid inclusions that contain liquid hydrocarbons were rarely

seen and only a small quantity of immiscible oil inclusions of special forms can be found in gypsum that was formed at later stage. As can be seen under transmission microscopy (Fig. 4-2,3), yellow spheroids in the form of double rings and black spheroids occur in the big spherical inclusions, and when H3 blue laser-excited fluorescence was applied to this field of vision, the spheroids in the form of double rings in the inclusions would show remarkable yellow fluorescence and refer to liquid hydrocarbon, the peripheral parts of the inclusions show weak yellowish green fluorescence and refer to water phases (containing soluble hydrocarbon), while the black spheroids show no fluorescence. When LIKAM-600 model stage was used for further temperature measurement, the inner rings of the double-ring spheroids would disappear at 89°C, hence referring to gaseous hydrocarbon phases, while the black spheroids show no remarkable variations. Laser Raman detection yields no positive results since the fluorescence shown by the inclusions is too strong.

4.2 Elemental sulphur-bearing immiscible inclusions

The solid phases in an inclusion trapped from a homogenized system generally refer to saline minerals closely related to metallogenic processes. However, a

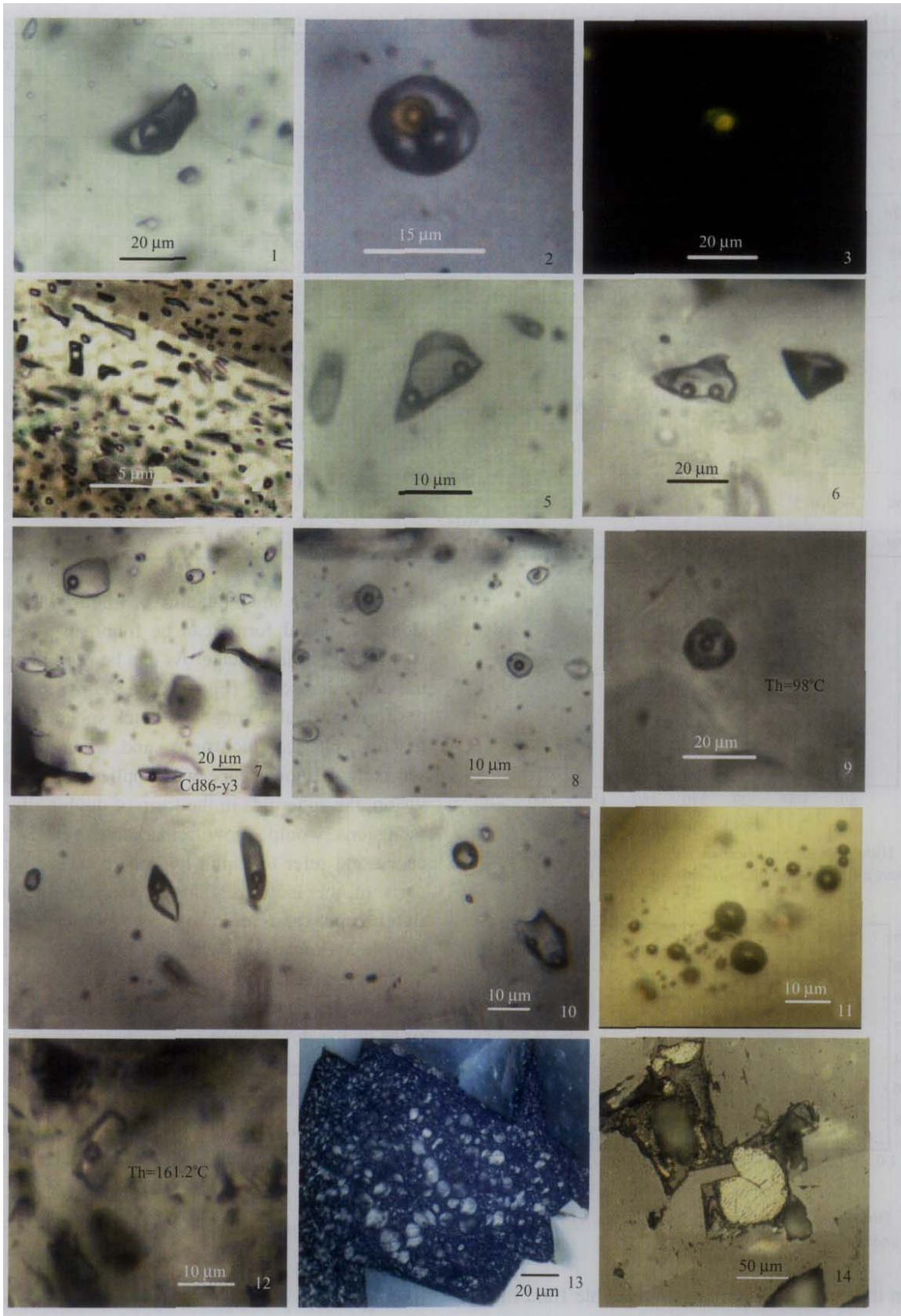


Fig. 4. Illustrations on inclusion photomicrographs. 1, 5, 6. The polyphase immiscible fluid inclusions trapped in authigenic gypsum in the T1f3-1 carbonate reservoir in Jinzhu 1 well contain two separate spheroids, one is gaseous H₂O, while the other was determined to be solid natural sulphur by laser Raman spectrometry. Transmitted light, 63×10. 2, 3. The hydrocarbon-bearing, polyphase immiscible fluid inclusions trapped in calcite in the T1f3-1 carbonate reservoir in Jinzhu 1 well are spheroidal in shape and big in size. The spheroidal, big-sized inclusion consists of one yellow, double-ring-shaped spheroid and one black spheroid. Under fluorescent microscope, the double-ring shaped spheroid shows yellow fluorescence and refers to liquid hydrocarbon and its peripheral water phase shows weak yellowish green fluorescence (indicating occurrence of soluble hydrocarbon), while the black spheroid shows no fluorescence. (2) Transmitted light, 63×10; (3) Fluorescent light, 25×10. 4. Solid bitumen and bitumen-bearing immiscible inclusions distributed in calcite in the T1f3-1 carbonate reservoir in LuoJia 2 well. Transmitted light, 20×10. 7, 8, 10. Double-spheroidal immiscible fluid inclusion groups distributed in authigenic gypsum in the T1f3-1 carbonate reservoir in Jinzhu 1 well. Transmitted light, 63×10. 9. The two-phase fluid inclusions trapped in authigenic gypsum in the T1f3-1 carbonate reservoir in Jinzhu 1 well show a homogenization temperature Th=98°C. Transmitted light, 32×10. 11. Gas inclusions contained in elemental sulphur (orthorhombic sulphur) in the T1f3-1 carbonate reservoir in Jinzhu 1 well. Transmitted light, 63×10. 12. High temperature fluid inclusions trapped in calcite in the T1f3-1 carbonate reservoir in Jinzhu 1 well show a homogenization temperature Th=161.2°C. Transmitted light, 32×10. 13. Reservoir bitumen with strongly inhomogeneous spherulitic inter-phase structure trapped in calcite of the T1f3-1 limestone in Tieshan 5 well. Reflected light with crossed nicols, 20×10. 14. Reservoir bitumen with spheroidal structure filled in calcite of the T1f3-1 carbonate geode in Tieshan 5 well. Reflected light, 20×10.

very special type of immiscible inclusions in the form of double-spheroid can be found in authigenic gypsum in gas reservoirs of the study area. As can be seen from Fig. 4-1, 5, 6, 7, 7, 9, 10, two spheroids separated from each other occur in inclusions of various shapes. Further observation indicates that one of the two spheroids can be mobile and got homogenized into liquid and finally disappeared when being heated on a stage, suggesting that it is a kind of gas bubble. Nevertheless, the other spheroid showed no change when being heated even to a very high temperature on the stage, and laser Raman spectrometric analysis suggests that it is the solid phase of elemental sulphur. For details please see Fig. 5, Fig. 6 and Fig. 7. For example, laser Raman analyses were carried out separately at the A, B, and C points as marked on the double-spheroidal immiscible inclusion in CD8660-1-5 sample (Fig. 5), and it can be seen from the laser Raman spectra corresponding to A1, A2, B1, B2, C1, C2 that the compositions at the three points are quite different from one another, here point A (big spheroid in the inclusion) shows strong peaks at 218, 472, 150 cm⁻¹, which are characteristic of sulphur (A1 in Fig. 5), and peak at 2569 cm⁻¹, which is representative of H₂S (A2 in Fig. 5). As to the peak at 2497 cm⁻¹, it is hard to assign to a particular compound. When the results were presented at the symposium dedicated to inclusions held in Beijing in 2004, this special peak attracted attention from Prof. Jacques Pironon, who reported that they had also found it in their latest research. Point B (small spheroid in the inclusion) basically shows no peaks that represent sulphur (B1 in Fig. 5), except peaks at 1000, 622 cm⁻¹ representative of

the host mineral gypsum, peak at 2917 cm⁻¹ is CH₄ (B2 in Fig. 5); Point C (water phase in the inclusion) shows not only a remarkable water peak at 3432 cm⁻¹, but also a peak at 2589 cm⁻¹ characteristic of HS⁻ in water. In addition, as shown in Fig. 6, cd86-47 sample shows a peak at 2917 cm⁻¹ that is characteristic of methane in the gas inclusion in gypsum (Fig. 6A). Cd86-7 sample shows peaks characteristic of elemental sulphur in inclusions trapped in calcite (Fig. 6B); cd86-14 and cd86-15 samples both show two distinct types of laser Raman peaks that correspond to the double-spheroidal immiscible inclusion in gypsum, here one of the test points shows peaks representative of elemental sulphur (Fig. 6C), while the other test point corresponds to gaseous H₂O, but only shows peaks characteristic of the host mineral gypsum (Fig. 6D). Similar to the case shown in Fig. 6, in Fig. 7 one of the small spheroids refers to elemental sulphur, while the other test point corresponds to gaseous H₂O. Being paragenetic with elemental sulphur-bearing immiscible inclusions as trapped in gypsum, salt-water inclusions and CH₄-bearing pure gas inclusions, *etc.* show a homogenization temperature of ca. 100°C.

Identification of laser Raman spectra as made above for fluid inclusions was mainly based on measurement of calibration samples and literature results. The Raman peaks at 216.4–217 cm⁻¹, 472–473 cm⁻¹, 149–152 cm⁻¹, 436–437 cm⁻¹ are characteristic of amorphous elemental sulphur-orthorhombic sulphur, while the peaks at 2497–2590 cm⁻¹ are characteristic of HS⁻ and H₂S in water^[9]; the peak at 2917 cm⁻¹ is characteristic of CH₄^[9]; the peaks at 999–1000 cm⁻¹ and at 1016–1019 cm⁻¹ are the major peaks referring

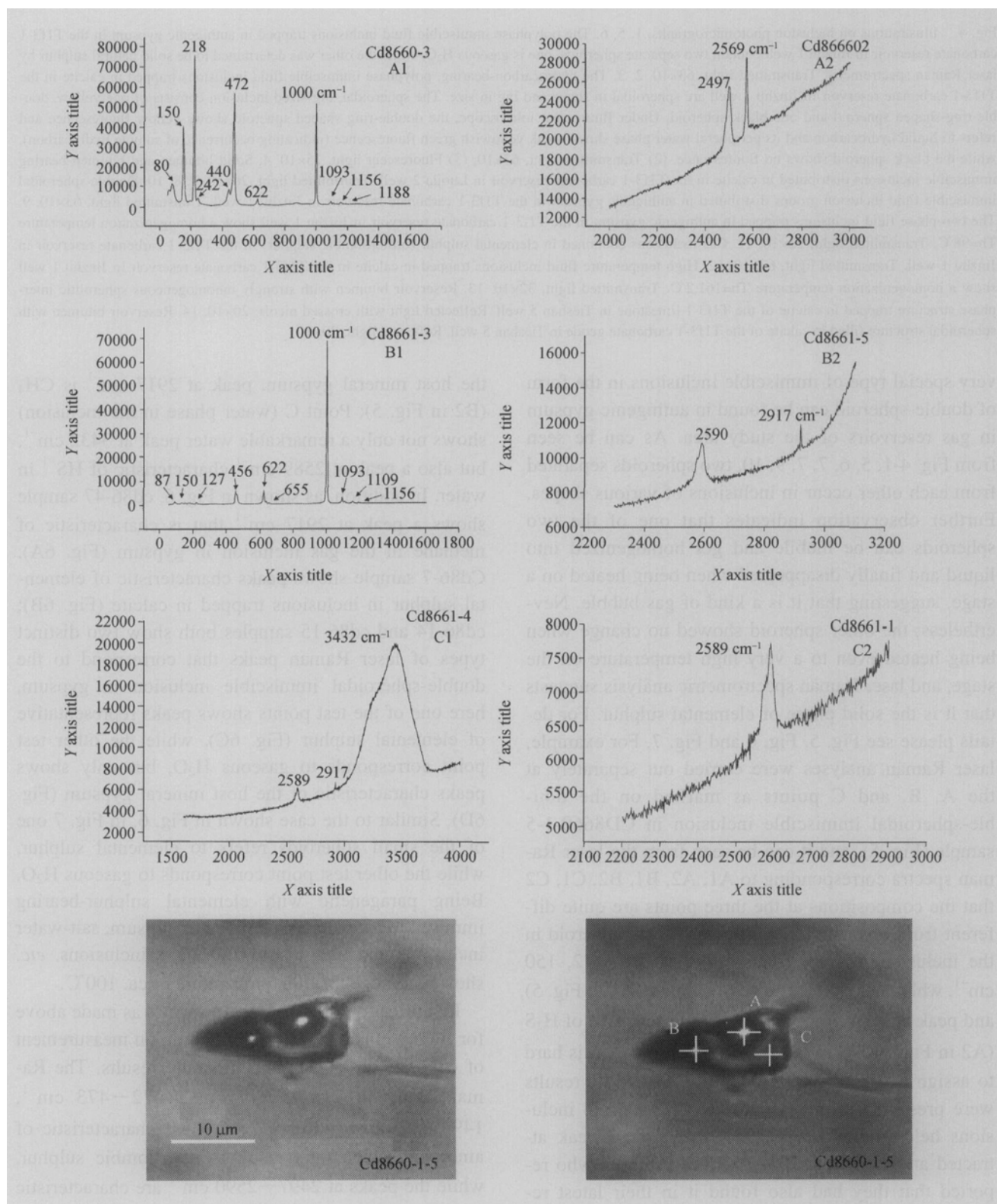


Fig. 5. Microscopic laser Raman spectra at points A, B, and C of an immiscible fluid inclusion.

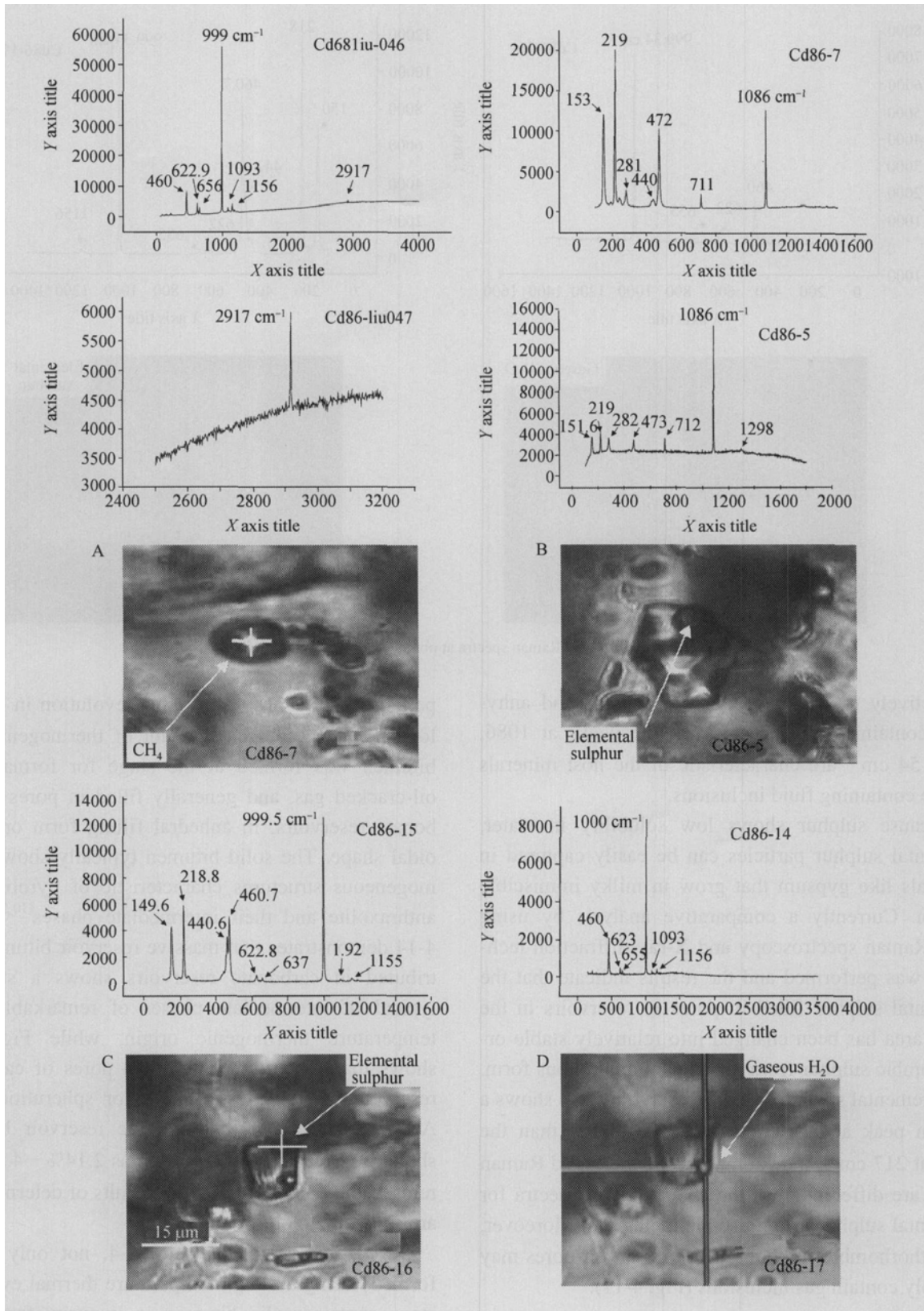


Fig. 6. Microscopic laser Raman spectra at points of an immiscible fluid inclusion.

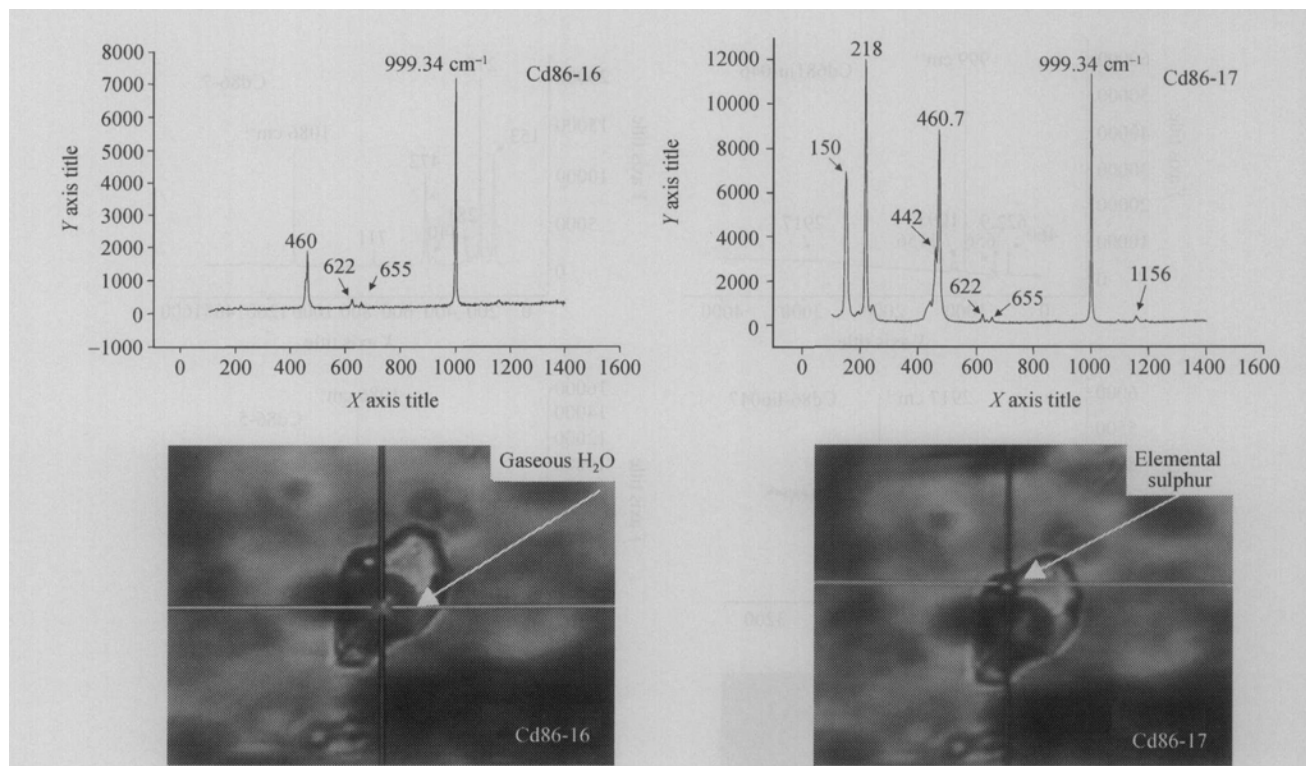


Fig. 7. Microscopic laser Raman spectra at points of an immiscible fluid inclusion.

respectively to the host minerals gypsum and anhydrite containing fluid inclusions; the peaks at 1086, 711, 154 cm^{-1} are characteristic of the host minerals calcite containing fluid inclusions.

Because sulphur shows low solubility in water, elemental sulphur particles can be easily captured in minerals like gypsum that grow in milky immiscible system. Currently a comparative analysis by using laser Raman spectroscopy and X-ray diffraction technique was performed and the results indicate that the elemental sulphur filled in pores in reservoirs in the study area has been changed into relatively stable orthorhombic sulphur from its original amorphous form. The elemental sulphur filled in reservoir pores shows a Raman peak at 471 cm^{-1} , which is higher than the peak at 217 cm^{-1} , indicating that the measured Raman peaks are different from the characteristic spectra for elemental sulphur in immiscible inclusions. Moreover, the orthorhombic sulphur filled in reservoir pores may possibly contain gas inclusions (Fig. 4-11).

4.3 Solid bitumen-bearing immiscible inclusions

Because the oolite reservoir underwent high tem-

perature (>170–180°C) thermal evolution in its geological history, a great amount of thermogenic solid bitumen was formed at the stage for formation of oil-cracked gas, and generally filled in pores of carbonate reservoirs, in anhedral filling form or spheroidal shape. The solid bitumen typically shows inhomogeneous structures characteristic of pyrobitumen-anthraxolite and their intermediate phases^[10,11]. Fig. 4-14 demonstrates that massive reservoir bitumen distributed in carbonate reservoirs shows a structure typical of intermediate phases of remarkable, high temperature thermogenic origin, while Fig. 4-13 shows that pyrobitumen filled in pores of carbonate reservoirs is in vein wall form or spherulitic form. Among the samples studied, the reservoir bitumen shows a reflectivity BR_0 as high as 2.14%–4.5% and remarkable double reflection. Results of determination are shown in Table 1 and Fig. 3.

As can be seen from Fig. 4-4, not only calcite formed during the high temperature thermal evolution stage contains solid bitumen in impurity forms, but also fluid inclusions contain solid bitumen in immiscible forms. This type of bitumen-bearing immiscible

inclusions records abundant information concerning crude oil at the high temperature pyrolysis stage.

4.4 Epigenetic immiscible inclusions

Since calcite, dolomite and anhydrite generally show fragile and soft properties, both organic and inorganic fluid inclusions originally captured from a homogenized system would undergo pyrolysis, polymerization, loss or scragging deformation, *etc.* in later stage thermal metamorphism and tectonic deformation, which would change the compositions and phases of the original system and transform the original fluid inclusions into epigenetic immiscible inclusions. As is shown from Fig. 4-4, black solid bitumen occurs in the walls of part of the high temperature inclusions that show relatively higher gas/liquid ratio of calcite, this is because liquid hydrocarbon in these inclusions would undergo thermal metamorphism at the stage of oil cracking in reservoirs, and be transformed into gas, and a great amount of gas would be left in the gaseous state, while a small amount of gas would be condensed into solid bitumen that would occur on the walls of high temperature inclusions.

4.5 Relationship between immiscible inclusions and homogeneous fluid inclusions

Immiscible inclusions are coexistent with homogeneous fluid inclusions in samples studied. Homogeneous fluid inclusions of gas/liquid phases predominate in calcite, while immiscible inclusions are mainly concentrated locally or distributed in a sporadic form in gypsum, which demonstrates that the fluids in hydrocarbon reservoirs are remarkably distinct from the ordinary petrogenic fluids and the metallogenic fluids for metallic hydrothermal ore deposits. Macroscopically, fluid in an oil/gas structure is a relatively complicated inhomogenized system, while in some localized sections or microscopic parts fluids can be of a single-phase that is at its temperature and pressure equilibrium. As a result, fluid inclusions may possibly be captured in newly formed minerals, at the enlargement edges or on pore-healing planes of minerals in a reservoir, and hence can be used as tools for measurement and estimate of the temperature and pressure conditions of the reservoir, while immiscible inclusions enriched in hydrocarbons and “boiling” inclu-

sions may be captured by minerals which were newly formed in oil-water-gas transition zones and during processes of hydrocarbon migration and pressure decrease.

5 Trapping temperature and pressure of fluid inclusions

The trapping pressure of oil inclusions is an important parameter that can reflect the depth and pressure for formation of hydrocarbon reservoirs, but is difficult to determine. Presently extrapolation of trapping pressure can be performed with multiple PVTX simulation and calculation software and related methods^[12-16]. In regard to the method employed for this work, the first step is to simulate and calculate the compositions of and saturation pressure for oil inclusions with PVTsim software and the method proposed by Aplin *et al.* in 1999^[12], while the second step is to further simulate and derive the isometric equation for oil inclusions and their paragenetic salt water inclusions and to calculate the trapping temperature and pressure for various types of oil inclusions, with PVTsim software and the method adopted by Liu *et al.* in 2003^[14].

Basic parameters utilized for PVTsim simulation and calculation for oil inclusions from Jinzhu 1 well are: homogenization temperature for oil inclusions = 98.1°C, gas/liquid ratio = 11.6%; (Since oil inclusions show spheroidal shapes similar to those of bubbles, their two dimensional image analytical data shall be similar to the CLSM-determined results). The compositions simulated and calculated for inclusions (mol%) are: (N₂=0.544, CO₂=3.450, C₁=49.605, C₂=5.326, C₃=3.596, iC₄=0.680, nC₄=1.604, iC₅=0.710, nC₅=0.846, C₆=1.115, C₇=2.653, C₈=3.169, C₉=2.080, C₁₀-C₁₃=6.532, C₁₄-C₁₆= 4.383, C₁₇-C₂₀=4.63, C₂₁-C₂₃= 2.821, C₂₄-C₂₆=2.146, C₂₇-C₃₁=2.509, C₃₂-C₃₆=1.600).

The saturation pressure for trapped oil inclusions through simulation and calculation is $P=274.15 \times 10^5$ Pa, and the isometric equation A derived for the oil inclusions is: $P=4.43t-159.99$. The salt-water inclusions paragenetic with trapped oil inclusions yield a homogenization temperature =105°C, a freezing point = -5.5°C, and an isometric equation B: $P=38.2t-3972$.

When the two equations A and B are solved together, the temperature and pressure for trapped oil inclusions are: $T_r=112.88^\circ\text{C}$, $P_r=340.07\times 10^5\text{Pa}$. Fig. 8 is a diagram that shows the evolution of phases in oil inclusions under different P-T conditions and the isometric lines for both oil inclusions and salt water inclusions (The isometric line for salt water inclusions as shown in the diagram refers to the line of simulation of the unsaturated system of methane in water)^[14-16]. As the oil inclusions are paragenetic with immiscible inclusions that contain elemental sulphur in the samples, the P-T conditions derived from oil inclusions can also be regarded as conditions for formation of the immiscible inclusions.

6 Discussion on the origin of hydrogen sulphide

In regard to the origin of H_2S in natural gas reservoirs, extensive research has been conducted by numerous scholars based on sulphur isotope composition data and experimental results of thermal reducing reactions between sulphates and hydrocarbons^[17-23]. It is generally agreed that H_2S in gas reservoirs in different areas could be related to three types of geological-geochemical processes, *i.e.*, (1) thermal disintegration of sulphur-bearing organic matter in kerogen; (2) bacterial reduction of sulphate minerals (BSR) in gypsum-bearing carbonate at a temperature of $<60-80^\circ\text{C}$; and (3) high temperature thermochemical reduction

between sulphate minerals in gypsum-bearing carbonate rocks and hydrocarbons (TSR)^[17,18].

Based on the close relationship between the H_2S -bearing gas reservoirs and the anhydrite-bearing carbonate rocks in the study area, the characteristic $\delta^{34}\text{S}$ of H_2S in natural gas ($+12\text{‰}-+13\text{‰}$ CDT) and the characteristic $\delta^{34}\text{S}$ of sulphate minerals ($+11\text{‰}-+21\text{‰}$, with a mean of $+15\text{‰}$ CDT), and geological-geochemical data such as the highest geothermal temperature of $>130^\circ\text{C}$ suffered by reservoir rock, *etc.*, previous scholars like Wang *et al.* (2002)^[8], Cai *et al.* (2003)^[21], Cai *et al.* (2004)^[22], and so on held that H_2S in natural gas reservoirs was mainly of TSR origin. In this paper the temperature, pressure and geological-geochemical conditions during the TSR processes of H_2S in natural gas reservoirs will be further discussed, based upon reflectivity of reservoir bitumen and homogenization temperature of fluid inclusions in the samples, and in particular the occurrence and distribution characteristics of immiscible inclusions that are enriched in elemental sulphur, H_2S and other components.

Formation of H_2S and elemental sulphur in natural gas reservoirs in the study area requires some basic conditions to be satisfied: In Luojiashai, Dukouhe and Tieshanpo at the two sides of the Kaijiang-Liangping trough, the Ertan gas reservoir in the Lower Triassic Feixianguan Formation contains 12%–17% of H_2S ,

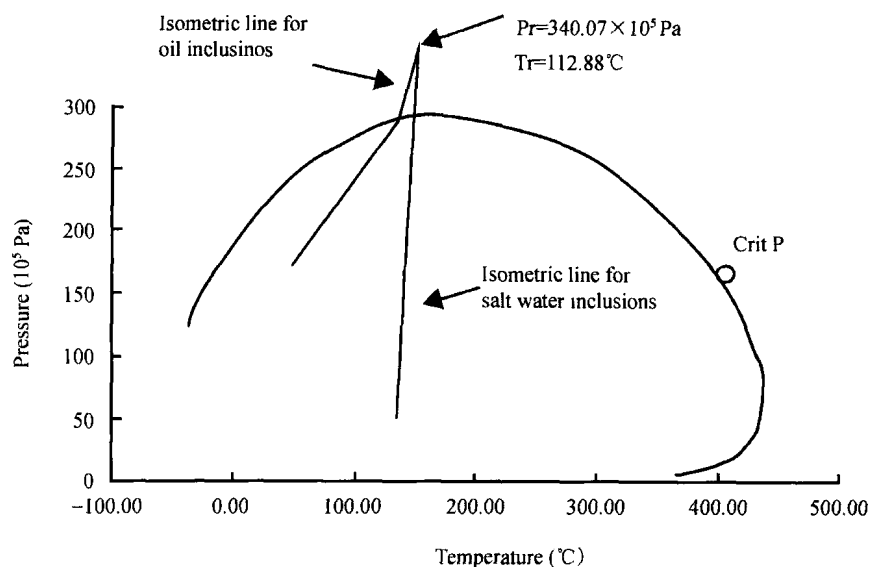


Fig. 8. Diagram showing evolution of phases in oil inclusions.

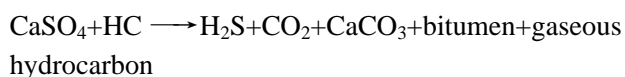
and the gas reservoir at Jinzhu is filled locally by natural sulphur (orthorhombic sulphur) of light yellow color. The burial history and thermal evolution history of gas reservoirs in the study area demonstrate that the greatest burial depth is more than 6,000 m and the highest paleogeothermal temperature is above 200°C^[7]. The measured reservoir bitumen in samples shows a reflectivity as high as 2.4%–4.1% and remarkable double reflection, and structures of pyrobitumen-anthracolite of pyrometamorphic origin and their special intermediate phases, and platy mosaic structures; The carbonate minerals in the reservoirs show three groups of homogenization temperatures for fluid inclusions: the homogenization temperature of fluid inclusions can be as high as 160°C–180°C in the stage for formation of oil-cracked gas, varies from 100°C–110°C in calcite formed at late stage after the reservoirs were uplifted; and mainly changes from 98°C–108°C in authigenic gypsum minerals. Multiple layers and blocks of anhydrite were developed in gas-bearing sections; calcite, anhydrite, gypsum, natural sulphur (orthorhombic sulphur) are extensively paragenetic with one another in reservoirs like Jinzhu 1 well; multiple types of immiscible inclusions that contain elemental sulphur and H₂S, *etc.* occur in late stage gypsum-anhydrite and calcite crystals.

Worden *et al.* (1995)^[19] and Machei (1998)^[18] thought that the temperature for TSR to occur in gas reservoirs is 140°C, while Worden and Smalley (2001)^[20] held that in some other hydrocarbon producing basins TSR may occur in 120–130°C. Still, Cai *et al.* (2003)^[22] and Cai *et al.* (2004)^[21] deemed that TSR mainly occurred at 130–140°C in the study area. The measured results of homogenization temperature of fluid inclusions and the characteristics of occurrence of immiscible inclusions that contain elemental sulphur and H₂S in gas reservoirs in the study area further demonstrate that H₂S in the reservoirs was mainly originated from thermochemical reaction between hydrocarbons and sulphates at the oil-cracked gas formation stage in Yanshannian and that elemental sulphur was derived from partial oxidation of H₂S and further reactions among sulphates, hydrocarbons and H₂S at the reservoir uplift stage in Himalayan. Major genetic models involved and associated temperature

and pressure conditions are listed as follows:

(1) The oil/gas reservoir underwent settlement and burial, at this stage H₂S was formed through the high temperature thermal fluid reaction as follows:

$$120^{\circ}\text{C} - 180^{\circ}\text{C}$$



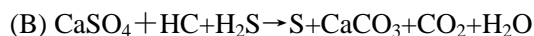
Also at this stage, the newly generated calcite trapped high temperature fluid inclusions, which contain H₂S-bearing gaseous hydrocarbons and solid bitumen.

(2) During the later stage of uplift of reservoirs and decrease in both temperature and pressure, elemental sulphur was formed according to the following reactions:

$$(95^{\circ}\text{C} - 105^{\circ}\text{C}) (340 \times 10^5 \text{Pa})$$



$$(95^{\circ}\text{C} - 105^{\circ}\text{C}) (340 \times 10^5 \text{Pa})$$



At this second stage, not only elemental sulphur was commonly generated in cracks and pores in reservoirs but also multiple types of sulphur-bearing immiscible inclusions were trapped in newly generated and recrystallized calcite and gypsum crystals.

The genetic models as described above demonstrate that in gas-bearing strata with gypsum and anhydrite interlayers, generation of H₂S can possibly continue in areas with burial depth greater than 5,000–4,000 m and temperature higher than 110°C–120°C, which will surely result in higher concentration of H₂S in the gas reservoir. However, in areas with no gypsum and anhydrite interlayers and burial depth less than 3,000 m, the H₂S concentration will generally be lower.

7 Conclusions

Results of laser Raman spectral analysis and fluorescence detection indicate that multiple special forms of immiscible inclusions that contain elemental sulphur, liquid hydrocarbons and bitumen, *etc.* occur in the carbonate reservoir samples collected from Jinzhu area. Fluid inclusions of multiple formation stages that show homogenization temperatures of 89°C–120°C, 130°C–160°C, and 170°C–180°C occur in dolomite and calcite minerals in gas reservoirs, and multiple

types of immiscible inclusions showing homogenization temperature of $85^{\circ}\text{C} - 95^{\circ}\text{C}$ occur in the later stage anhydrite-gypsum and calcite. Based on the reflectivity of reservoir bitumen (2.4%–4%), the stage with maximum burial depth, the homogenization temperature of fluid inclusions (being as high as $170^{\circ}\text{C} - 180^{\circ}\text{C}$), and the fact that the gas-producing section is enriched in gypsum and anhydrite interlayers, it can be inferred that the oolite gas reservoir in the Triassic Feixianguan Formation in East Sichuan resulted from oil-cracking, the H_2S in gas reservoirs was mainly of TSR origin, *i.e.*, originated from the thermal reaction between hydrocarbons in hydrocarbon-bearing reservoirs and CaSO_4 in the gypsum-bearing strata at the high temperature ($140^{\circ}\text{C} - 170^{\circ}\text{C}$) oil cracking and gas formation stage in Cretaceous, and the elemental sulphur-orthorhombic sulphur in the reservoirs was derived from the partial oxidization of H_2S and further reaction among sulphates, hydrocarbons and H_2S in geological fluids in hydrocarbon-bearing reservoirs at a temperature of $85^{\circ}\text{C} - 89^{\circ}\text{C}$ during the regional uplifting and subsequent temperature decrease and pressure decrease stage in Himalayan. Meanwhile, gypsum-anhydrite formed at this stage and calcite formed at the later stage captured multiple kinds of immiscible inclusions that contain natural sulphur, *etc.* The multiple forms of fluid inclusions that occur in gas reservoirs reflect the complexity of the evolution of fluids in the study area and the origin of H_2S and elemental sulphur in gas reservoirs.

Acknowledgements This research was supported by the State Brainstorm Science Program for the Tenth Five-Year Plan Period (Grant No. 2001BA605A-0404) and the Frontier Research Program Sponsored by Guangzhou Institute of Geochemistry of Chinese Academy of Sciences (Grant No. GiGCX-04-08).

References

1. Shepherd, T. J., A practical guide to fluid inclusion study, New York: Blackie, Chapman & Hall, 1985, 35–136.
2. Liu Dehan, Inclusion study, a powerful tool for tracing fluids in basins, *Geoscience Frontier* (in Chinese), 1995, 4(4): 149–153.
3. Lu Huanzhang, Li Dinglun, Shen Kun *et al.*, Inclusion geochemistry (in Chinese), Beijing: 1990, 61–115.
4. Lu Huanzhang, Fan Hongrui, Ni Pei *et al.*, Fluid Inclusions (in Chinese), Beijing: Science Press, 2004, 17–202.
5. Liu Bin, Shen Kun, Thermodynamics of Fluid Inclusions (in Chinese), Beijing: Geological Publishing House, 1999, 12–16.
6. Liu Dehan, Xiao Xianming, Jia Rongfen *et al.*, Observation of hydrocarbon generation and migration of highly-matured carbonate by means of laser-induced fluorescence microscopy, *Chinese Science Bulletin*, 2000, 45(suppl.): 16–20.
7. Wang Yigang, Chen Shengji, Xu Shiqi, Formation Conditions and Exploration Technologies for Gas Reservoirs in Paleozoic-Upper Proterozoic in Sichuan Basin (in Chinese), Beijing: Petroleum Industry Press, 2001, 1–7.
8. Wang Yigang, Dou Lirong, Wen Yingchu *et al.*, Study of origin of H_2S in high sulphur-bearing gas reservoirs in Triassic Feixianguan Formation in northeastern Sichuan Basin, *Geochimica*, 2002, 31(6): 1–7.
9. Emst, A., Burke, J., Raman microspectrometry of fluid inclusions, *Lithos.*, 2001, 55: 139–158.
10. Liu Dehan, Lin Maofu, Discovery of small vanadium and nickel minerals from anthraxolite and discussion of their origin, *Scientia Sinica, Series B*, 1983, 27(11): 1197–1202.
11. Liu Dehan, Application of bitumen in carbonate in study of hydrocarbon generation and evolution and formation of metallic ore deposits, in GIGCAS (ed.), Paper Collection on Organic Geochemistry, Beijing: Science Press, 1986, 133–138.
12. Aplin, A. C., Mcleod, G., Larter, S. R. *et al.*, Combined use of confocal scanning microscopy and PVT simulation for estimating the composition and physical properties of petroleum in fluid inclusion, *Marine and Petroleum Geology*, 1999, 16:97–110.
13. Aplin, A. C., Larter, S. R., Bigge, M. A. *et al.*, PVTX history of the North Sea's Judy oilfield, *Journal of Geochemical Exploration*, 2000, (69–70): 641–644.
14. Liu, D. H., Xiao, X. M., Mi, J. K. *et al.*, Determination of trapping pressure and temperature of petroleum inclusion using PVT simulation inclusion of lower Ordovician carbonates from the Lunnan low uplift, Tarim Basin, *Marine and Petroleum Geology*, 2003, 20: 29–34.
15. Mi Jingkui, Xiao Xianming, Liu, Dehan *et al.*, Determination of paleo-pressure for a natural gas pool formation based on PVT characteristics of inclusion in reservoir rock — A case study of Upper-Plaeozoic deep basin gas trap of Ordos Basin, *Science in China, Series D*, 2004, 47(6): 507–513.
16. Teinturier, S., Pironon, J., Walgenwitz, F., Fluid inclusion and PVTX modeling: Examples from the Garn Formation well 6507/2-2, Haltenbanken, Mid-Norway, *Marine and Petroleum Geology*, 2002, 19: 755–765.
17. Machei, H. G., Krouse, H. R., Sassen, R., Products and distinguishing criteria of bacteria and thermochemical sulfate reduction, *Applied Geochemistry*, 1995, 10: 373–389.

18. Machei, H. G., Gas souring by thermochemical sulfate reduction at 140°C: Discussion, AAPG Bull., 1998, 82(100): 1870—1873.
19. Worden, R. H., Smalley, P. C., Oxtoby, N. H., Gas souring by thermochemical sulfate reduction at 140°C, AAPG Bulletin, 1995, 79(6): 854—863.
20. Worden, R. H., Smalley, P. C., H₂S in North Sea oilfield: Importance of thermochemical sulfate reduction in clastic reservoirs, The Proceedings of the 10th International Symposium on Water-Rock Interaction, Vol. 2, Balkema, Lisse, 2001, 659—662.
21. Cai, Chunfang, Worden, R. H., Bottrell, S. H. *et al.*, Thermochemical sulphate reduction and the generation of hydrogen sulphide and thiols (mercaptans) in Triassic carbonate reservoirs from the Sichuan Basin, China, Chemical Geology, 2003, 202: 39—57.
22. Cai, Chunfang, Xie, Zengye, Worden, R. H. *et al.*, Methane-dominated thermochemical sulphate reduction in the Triassic Feixianguan Formation in East Sichuan Basin, China: Toward prediction of fatal H₂S concentrations, Marine and Petroleum Geology, 2004, 21: 1265—1279.
23. Cross, M. M., Manning, D. A. C., Bottrell, S. H. *et al.*, Thermochemical sulphate (TSR): Experimental determination of reaction kinetics and implication of the observed reaction rates for petroleum reservoirs, Org. Geochem., 2004, 35: 393—404.